

BIAXIAL AND UNIAXIAL FATIGUE LIFE PREDICTION FOR  
AUSTENITIC STAINLESS STEELS SPECIMENS AND COMPONENTS

Leonardo BERTINI(\*) and Emilio VITALE(\*)

(\*) Dipartimento di Costruzioni Meccaniche e Nucleari  
University of Pisa

Third International Conference on  
Biaxial/Multiaxial Fatigue

April 3-6, Stuttgart, FRC

Summary

The paper presents the results obtained via the application of three creep-fatigue damage models, namely the "Continuous Damage Model", the "Damage Rate Approach" and the "Time and Cycle Fraction Summation" method, to the prediction of the number of cycles to failure observed in about 170 creep-fatigue tests conducted on AISI 304 and 316 stainless steel specimens at temperatures ranging from 550 to 650 °C. The data, obtained either from technical literature or from experimental work previously carried out by the authors, include a rather wide variety of stress/strain states (uniaxial, in-phase and out-of-phase biaxial) and of loading histories (tensile and compressive hold times, positive and negative "sawtooth" waveforms, etc.).

Material parameters required for model applications have been derived from about 2000 independent creep and creep fatigue tests contained in a purposely designed Material Data Base.

The statistical distribution of the ratio between predicted and observed cycles to failure have been studied, finding out differences between the three models and some loading conditions were creep-fatigue failure seems not to be adequately predictable. Some possible improvements to present life prediction methodology are finally suggested.

List of symbols

a	length of a fatigue crack	N	number of loading cycles
c	creep cavity size	$N_f$	number of cycles to fatigue failure
D, D <sub>C</sub> , D <sub>F</sub>	total, creep and fatigue damages	$\sigma$	stress

$\epsilon_p, \dot{\epsilon}_p$	plastic strain and strain rate	$\sigma_H$	hydrostatic stress
t	time	$\sigma_{eff}$	Von Mises stress
$t_f$	time to creep rupture	$\sigma_1$	maximum principal stress
$\epsilon_{eff}$	maximum plastic shear strain range		
$\epsilon^n$	normal strain range acting on the plane of maximum shear strain range	$\mu = \frac{\epsilon^n}{\epsilon_{eff}}$	$\mu' = \frac{\sigma_H}{\sigma_{eff}}$
		$\Gamma = \frac{\sigma_1}{\sigma_{eff}}$	

### Introduction

The prediction of creep-fatigue endurance for actual structural components gives rise to the problem of deriving and applying theoretical tools and evaluation procedures capable of offering a rather reliable prediction of material life under conditions which may significantly differ from those commonly employed for testing, such as multiaxial stress fields, complex loading histories and very long term effects. In such a field, a significant role may be played by the many creep-fatigue interaction models which have been proposed since the earlier '70s (see [1,2] for reviews), some of which could, at least from a conceptual viewpoint, take a full account of the previously mentioned effects.

To date, several independent comparative studies of the capabilities offered by some of these models are available [3-6], most of which are concerned with the prediction of the material endurance observed in uniaxial tests under rather complex strain waveforms (positive and negative sawtooth tests, compressive hold times) or loading histories (sequential creep-fatigue tests, two-strain-levels fatigue). Results obtained in these studies did not show any significant difference between the capabilities of single models, nor allowed enough confidence to be achieved concerning their behaviour under many conditions representative of actual components operation.

The present study was conducted with the purpose of contributing to the set up of a more sound basis for a quantitative evaluation of the present status-of-the-art in life prediction methodologies. Particularly, the work was focused to check the performances of three creep-fatigue interaction models, namely the "Continuous Damage Model" (CDM) [7], the "Damage Rate Approach" (DRA) [8] and the "Time and Cycle Fractions Summation" method (TCFS), for life prediction under several different loading conditions, also involving multiaxial stress/strain states; some uniaxial and biaxial creep-fatigue test results obtained at the Department of

Nuclear and Mechanical Construction (DCMN) of Pisa on welded model structures were also included as nearly representative of actual component behaviour. The first two models were selected as particularly suitable, from a theoretical viewpoint, when dealing with multiaxiality and/or nearly general loading histories, while the third model, being presently used by the ASME Code Case N47 [9] and by the RCC-MR [10], provided a significant comparison tool, representative of the present design practice.

### Models summary

Present design rules make generally use (even if with different application procedures) of a linear damage interaction and cumulation rule, namely the method, which may be summarized by the following relationship:

$$D_F + D_C = D \quad (1)$$

where the fatigue ( $D_F$ ) and creep ( $D_C$ ) damages are given by:

$$D_F = \sum \frac{N_i}{N_{fi}} \quad (2)$$

$$D_C = \int \frac{dt}{t_f} \quad \text{or} \quad \sum \frac{t_i}{t_{fi}} \quad (3)$$

The method derives from the Miner and Robinson approaches, developed respectively for fatigue and creep, and was presented by Taira [11] in the early '60s.

For applications involving AISI 304 and 316 stainless steels a safety area in the plane ( $D_F$ ,  $D_C$ ) is defined both by ASME and RCC-MR rules. According with this approach, total damages  $D$  at failure may range from 0.6 to 1, as a function of  $D_F/D_C$ . It was ascertained that experimental data may fall relatively far from the boundary of this area, both on the safe and on the unsafe sides [12].

The two other creep-fatigue interaction models considered in the present work, namely the CDM and the DRA, involve rather complex mathematical relations. For the sake of brevity, only the general features of these models will be herein outlined, while more detailed descriptions may be found in given references.

The CDM, first proposed by Lemaitre and Chaboche [7], was subsequently subjected to various improvements, mainly at French ONERA, and to several applications and validations [3,13,14].

The method is based on the assumption that material damage evolution may be described by a macroscopic parameter  $D$ , which, following Kachanov [15], is defined in terms of working area reduction. The creep-fatigue damage cumulation is described by means of the following relationship :

$$dD = d[D_C(D, A_C, r, k, \sigma_c)] + d[D_F(D, \beta, M_0, a, b, \sigma_1, \sigma_u, \sigma_{eq})] \quad (4)$$

which predicts nonlinear interaction between creep and fatigue and nonlinear damage cumulation in multilevel pure creep or fatigue tests. Failure is expected when the damage  $D$ , which is zero for the virgin material, reaches unity.

In equation (4),  $A_C$ ,  $r$ ,  $k$ ,  $\beta$ ,  $M_0$ ,  $a$ ,  $b$ ,  $\sigma_1$ ,  $\sigma_u$  are material parameters which are functions of temperature,  $\sigma_{eq}$  is the equivalent stress according to the Sines and Crossland criterion and  $\sigma_c$  is a creep equivalent stress, according to the Hayhurst formulation [16]. A recent version of the model [17] involving anisotropic damage evolution was not applied in the present work due to difficulties concerning material constants evaluation.

The Damage Rate Approach (DRA) was first proposed by Majumdar and Mayia in the middle 1970s and later extended to cover creep-fatigue interaction [8] and multiaxial stresses [18]. Damage evolution is modelled by the growth of preexisting or early-nucleated fatigue cracks and creep cavities from an initial size ( $a_0$  or  $c_0$ ) up to a critical size ( $a_c$  or  $a_c$ ). The rates of cracks and cavities growth are assumed to be given by :

$$\frac{1}{a} \frac{da}{dt} = F(C, A(\mu, \mu'), m, k, T/C, A_g, \epsilon_{eff}, \dot{\epsilon}_{eff}) \quad (5)$$

$$\frac{1}{c} \frac{dc}{dt} = G(C_g(\mu, \Gamma), k_c, m, \epsilon_{eff}, \dot{\epsilon}_{eff}) \quad (6)$$

In equations (5,6)  $A$ ,  $m$ ,  $k$ ,  $T/C$ ,  $k_c$ ,  $A_g$ ,  $C_g$  and the ratios  $a_c/a_0$  and  $c_c/c_0$  are material constants and functions whose values are temperature dependent, while  $\mu$ ,  $\mu'$  and  $\Gamma$  are parameters used to model multiaxial stress states and to distinguish between tensile and compressive loadings. According to this formulation, fatigue life is reduced by creep damage, while the opposite is not true. The model predicts nonlinear creep-fatigue interaction and linear damage cumulation in multilevel pure creep and pure fatigue tests.

### Life prediction methodology

Material parameters required by the CDM and the DRA were obtained making use of a Material Data Base (MDB), set up at the DCMN [19,20] and containing some thousands of fatigue, creep and creep-fatigue test data for AISI 304 and AISI 316 Stainless Steels at temperatures ranging between 430 and 750 °C. Whenever available, stress-strain quantities at stabilized cycles were employed.

Fatigue parameters for the CDM have been obtained by least square fitting of uniaxial tensile/compressive test results conducted under triangular loading waveform at strain rates high enough to avoid creep effects (strain rate  $\geq 4 \cdot 10^{-3} \text{ s}^{-1}$ ). For the DRA, lower strain rates data were also employed, since equation (5) explicitly includes the strain rate dependence.

Material parameters for creep have been derived in a similar way, using stress/time to rupture data. For the DRA, stress vs. steady-state creep rate data were also employed, as equation (6) does not directly account for stress effects.

As far as multiaxiality is concerned, the CDM allows predictions to be achieved based only on uniaxial results, while DRA requires the definition of the two parameters A and  $C_g$  as functions of  $\mu$  and  $\Gamma$ . In the present work, the following relationships were employed for these parameters, based on their dependence on the stress/strain states as reported in [18]:

$$A = A_0 \cdot ( 3.33 - 3 \cdot e^{-0.2513 \cdot \mu} )$$

$$G = G_0 \cdot \Gamma \quad \text{for } \Gamma > 0$$

$$G = 0 \quad \text{for } \Gamma < 0$$

where  $G_0$  and  $A_0$  are values pertaining to the uniaxial case. It was further assumed that temperature dependence could be modelled by  $A_0$  and  $G_0$  variations only.

It must be emphasized that, both for the CDM and for the DRA, results of special, purposely-designed tests would have been required to derive material parameters. In order to overcome the lack of these data, it was necessary to make use of some simplifying assumptions, also following the suggestion of the authors. A detailed description of the procedure employed is reported in [21].

Since a comparison with the current design methods was desired, creep and fatigue reference curves for application of the TCFS

method were drawn from the design curves of the ASME CCN47-23, by eliminating the built-in safety factors and by appreciating an average creep strength from minimum curves, as suggested by RCC-MR.

A higher level Data Base was set up, collecting material parameters for the three models and for different temperatures. This Data Base can be directly accessed by computer programs devoted to life prediction.

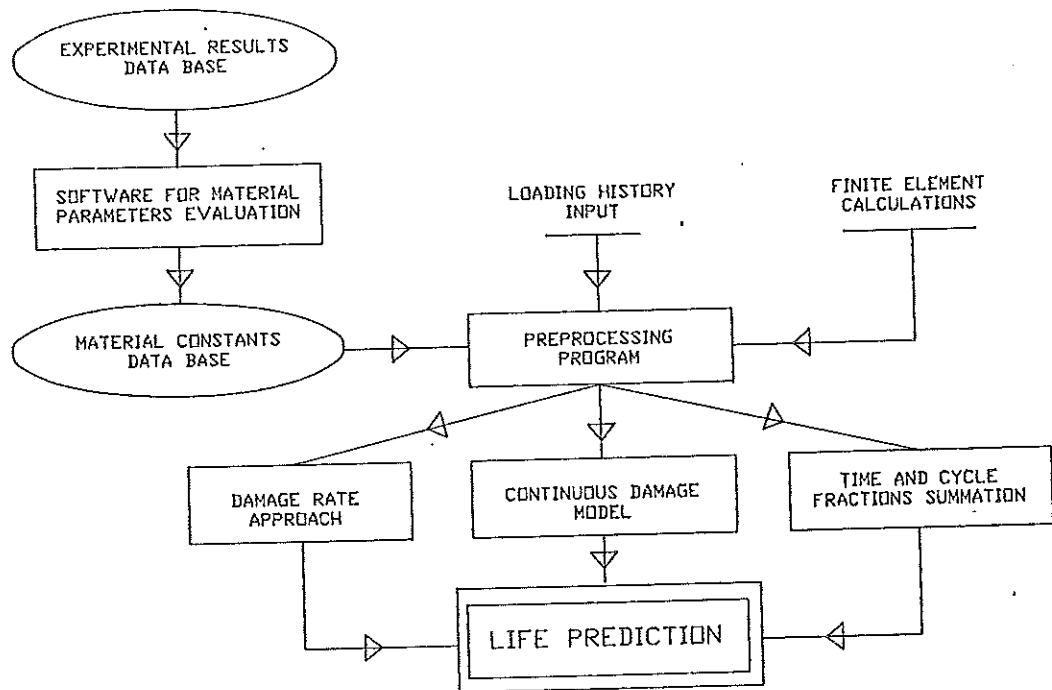


Fig.1 - General organization of the life prediction software

A computer program was developed, which allows for an interactive introduction of basic experimental data to be used for life prediction. This program can deal with uniaxial and multiaxial data, and evaluates the components of the stress/strain tensors which are not directly available from commonly reported experimental data. To this end, either built-in or user-specified cyclic stress-strain relationships may be chosen.

Information about the stress/strain history may then be alternatively employed by three FORTRAN-77 computer programs, which were developed for the application of the CDM, the DRA and the TCFS models. These programs may also be employed as post-processors of MARC and DCMN own MAVIS [22] Finite Element Codes, allowing structural integrity and life evaluations to be easily achieved at a design stage.

A detailed description of the software may be found in [23,24],

while Fig. 1 illustrates the general pattern of the life prediction methodology.

### Applications

The experimental data employed for the applications, where either drawn from published works and internal laboratory reports [25,34] or obtained at DCMN in the framework of research activities performed in the last decade [35]. All data were carefully selected as to be fully independent from those employed in deriving material parameters for the prediction models. According to the type of loading, they belong to the following main groups:

- uniaxial loading
- axial loading superimposed to constant internal pressure
- axial and torsional loading acting in phase
- axial and torsional loading acting alternatively

From the point of view of the loading waveform, available data can be classified in the following way:

- triangular continuous cycling (strain rates ranging from 0.0005 to 0.004 sec<sup>-1</sup>)
- other strain waveforms: cyclic strain with tensile or compressive hold times (duration up to 24 hours) and fast-slow and slow-fast cycles (negative and positive sawtooth waveform, respectively)
- complex loading histories: cyclic strain with hold time alternated with continuous cycling (in the following : "Complex Loading History 1" - CLH1) and cyclic strain with continuous cycling superimposed to tensile hold periods ("Complex Loading History 2" - CLH2).

A summary of available creep-fatigue test conditions is given in Table I (see [25] for more details on small specimens data sources).

Data from [28,29] were obtained on 12 mm diameter, 1.5 mm thickness tubular specimens, in which a small (1 mm diameter) hole was drilled at the mid gage length, in order to obtain a fixed location for crack initiation. Due to the presence of the notch and since only nominal values of stress and strain ranges were available, these data could not be directly compared with those obtained making use of smooth specimens. In the present analysis nominal stress and strain ranges have been adjusted, by constant stress and strain notch factors, in order to achieve a reasonable

fit of triangular continuous cycling test results. By this technique the effect of the notch has been virtually eliminated (for what concerns predictions comparison) and a significant number of data with complex loading histories and multiaxial stress states could be added to the small-size specimens data-set.

The DCMN data were obtained between 1979 and 1985 on 2 inches tubular welded specimens (see Fig.2), and were included in the present study as representative of the effects of all the main factors, such as welding technology and consequent notch effects, surface roughness, assembling tolerances, which differentiate structural behavior from laboratory test results.

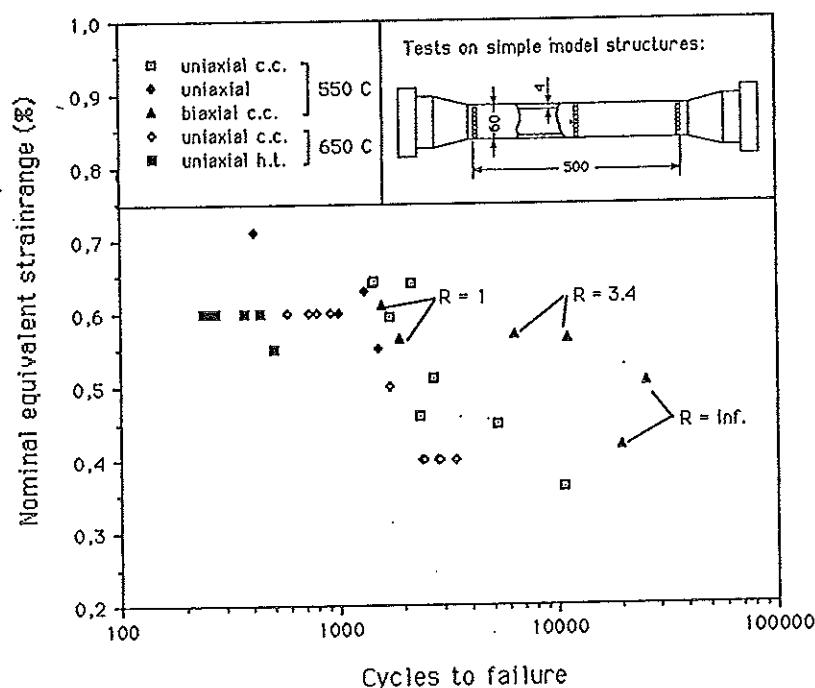


Fig.2 - Summary of test results for simple model structures

The experiments were conducted with triangular strain waves at strain rates of  $0.001 \text{ sec}^{-1}$  and temperatures of 550 and 650°C, with either uniaxial or biaxial (push-pull plus in-phase torsion) loads with torsional to axial strain ratios (R) of 1, 3.4 and infinity (see Fig. 2); some uniaxial tests were also conducted including a 0.05 hours hold-time at the maximum tensile strain. Details of these experiments can be found in [35].

The life of the model structures may be in principle predicted by evaluating the peak local strain and stress at the most critical point, which generally coincides with a weld root, at the boundary between weld and base materials. Local peak values can be evaluated by either a detailed (Finite Element) inelastic analysis or some simplified method, such as the Neuber rule. For the



present calculations the first method was employed for biaxial tests, where the application of simplified methods is not straightforward. For all the uniaxial tests the Neuber rule was applied, along with the experimentally derived cyclic stress strain curves [36] and an elastic FE evaluation of stress concentration factors at welds. As it is well demonstrated by many published results this procedure is quite accurate for uniaxial loads.

Since weld cross-section shapes could vary from one specimen to another and, within a single circumferential weld, between different locations, weld "best" and "worst" shapes were defined through examination of several joint sections. Then, each life prediction method was applied two times for each test in order to obtain upper and lower bound life predictions, respectively corresponding to the best and the worst weld shapes.

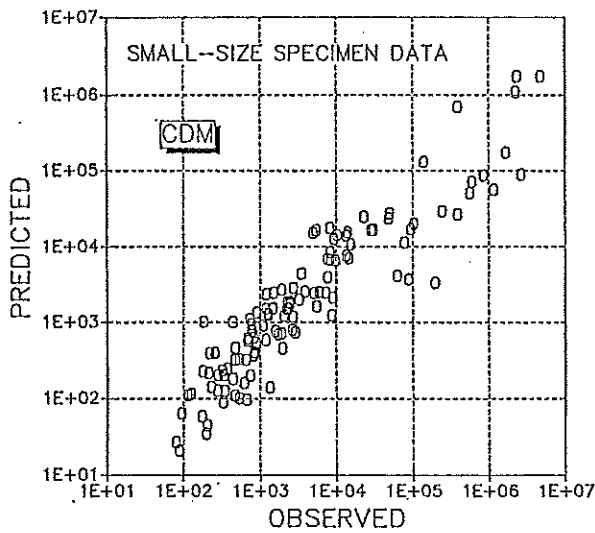


Fig.3

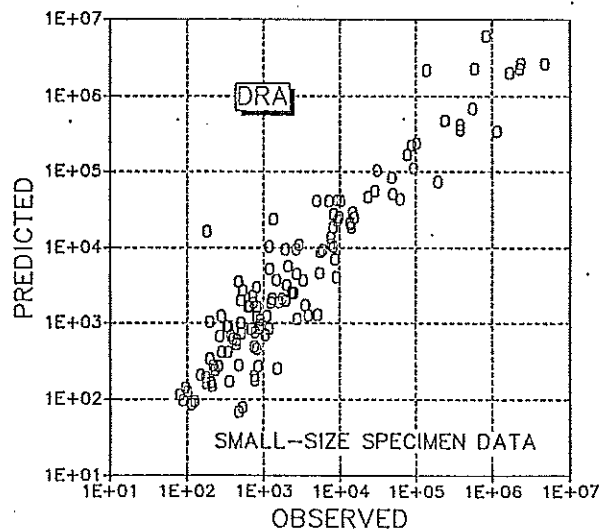


Fig.4

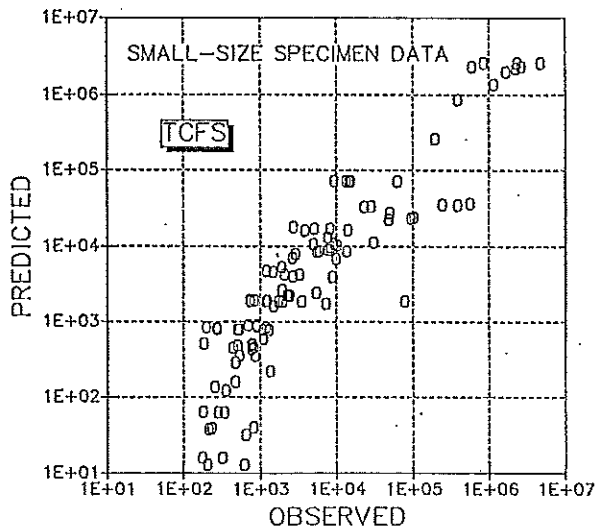


Fig.5

Figs.3,4,5 - Predicted vs. observed lives for small-size specimens.

### Results and discussion

Results obtained by the three models for all the available data on small (both smooth and notched) specimens are drawn in Figs. 3-5 as predicted versus observed cycles to failure. As a general trend, results are affected by a considerable scatter, which appears to be nearly constant along the observed fatigue life. The DRA shows a tendency toward a lower conservatism as compared to the other models. Figs. 6-8 show a similar comparison for tests on model structures: it is seen that predictions based on best and worst weld shapes represent an upper and, respectively, a lower bound that in many cases include the actual specimen life. There is however a definite trend for the DRA and the TCFS to produce more accurate predictions when worst weld shapes are used; on the other hand the CDM is generally more conservative and better forecasts are obtained when the lower notch effect is considered.

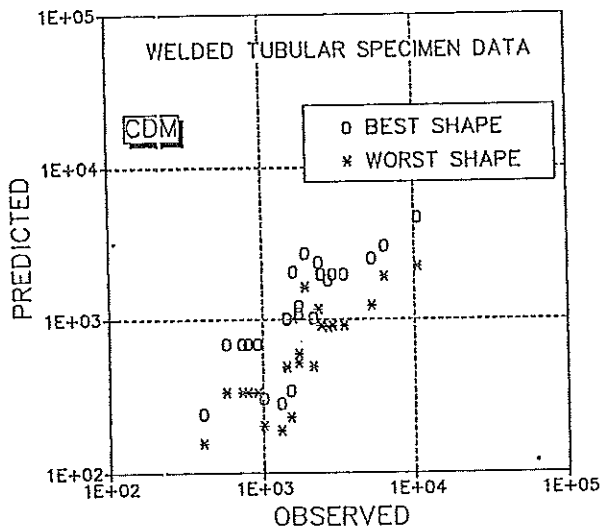


Fig.6

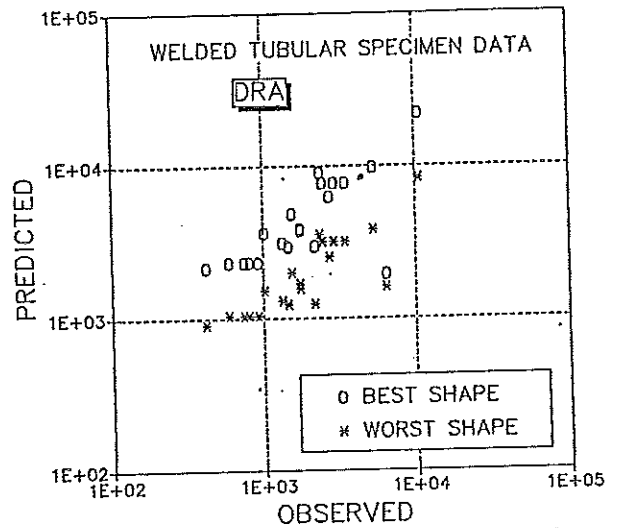


Fig.7

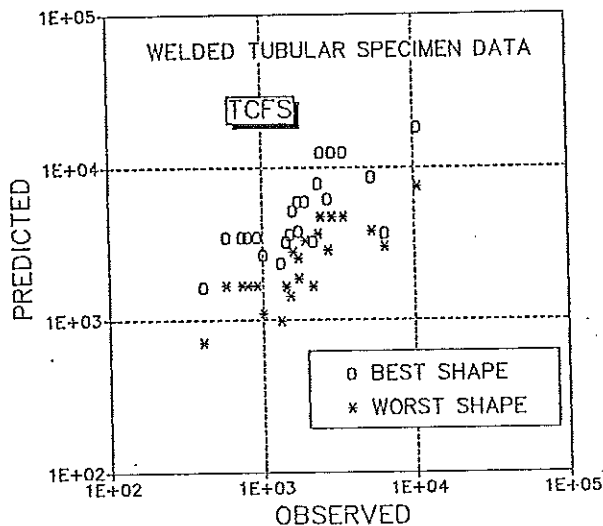


Fig.8

Figs.6,7,8 - Predicted vs. observed lives for model structures.

In order to achieve a better comparison of the three models, the statistical distributions of the ratio between predicted and observed cycles to failure were examined. The distribution obtained for small specimens under triangular waveform and continuous cycling is shown in Fig. 9: it is found that for this simple condition all of the models gave a most probable value of the representative ratio which is close to unity, the probability of a correct prediction (within a factor of 1.5) being more than 50%. This assures that a good correspondence exists between the parameters contained in the Data Base and the average behaviour of the tests being examined. The "queue" of extremely conservative results given by CDM and TCFS concerns a few high-strain/low-life data (observed cycles to failure less than 200).

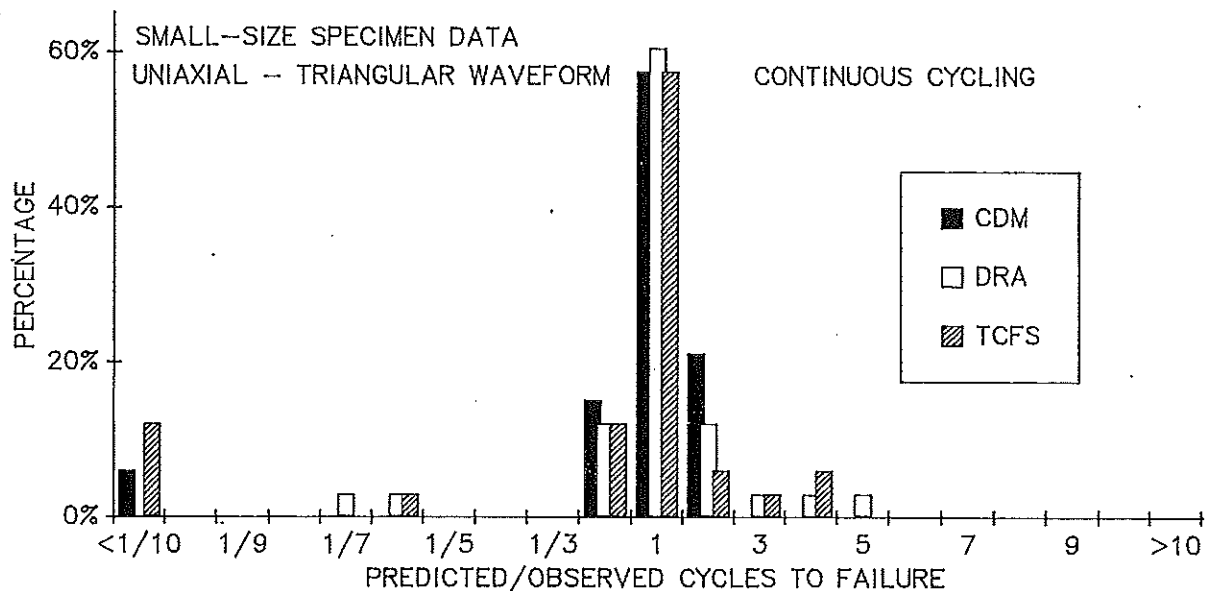


Fig.9 - Normalized distribution of predicted to observed life ratios.

The distribution obtained for small-size specimens and loading histories different from continuous cycling (including non-triangular strain waveforms and complex loading histories), depicted in Fig. 10, shows a significant increase in scatter for all the models. The most probable value is still close to unity for TCFS and DRA, while it decreases to 0.5 for the CDM. The highly unconservative results (representative ratios  $\geq 10$ ) shown for the TCFS and DRA models, are related with CLH2 data. The same is true for some of the highly conservative results given by the CDM. In addition, the TCFS gave very conservative results for some of the CLH1 data.

The effect of biaxial loading on prediction distributions for small-size specimens (including the in-phase continuous cycling

data and the axial-loading/internal-pressure data) can be observed in Fig. 11. Also for these data a significant increase of the scatter level is observed in comparison to data in Fig. 9, even if highly incorrect predictions seem to be less frequent than for uniaxial complex loading histories (Fig. 10). For the DRA the most probable value of the ratio between predicted and observed cycles to failure is less conservative than in the uniaxial tests (close to 2 instead of 1), while the most probable performance for the CDM and the TCFS is still near unity.

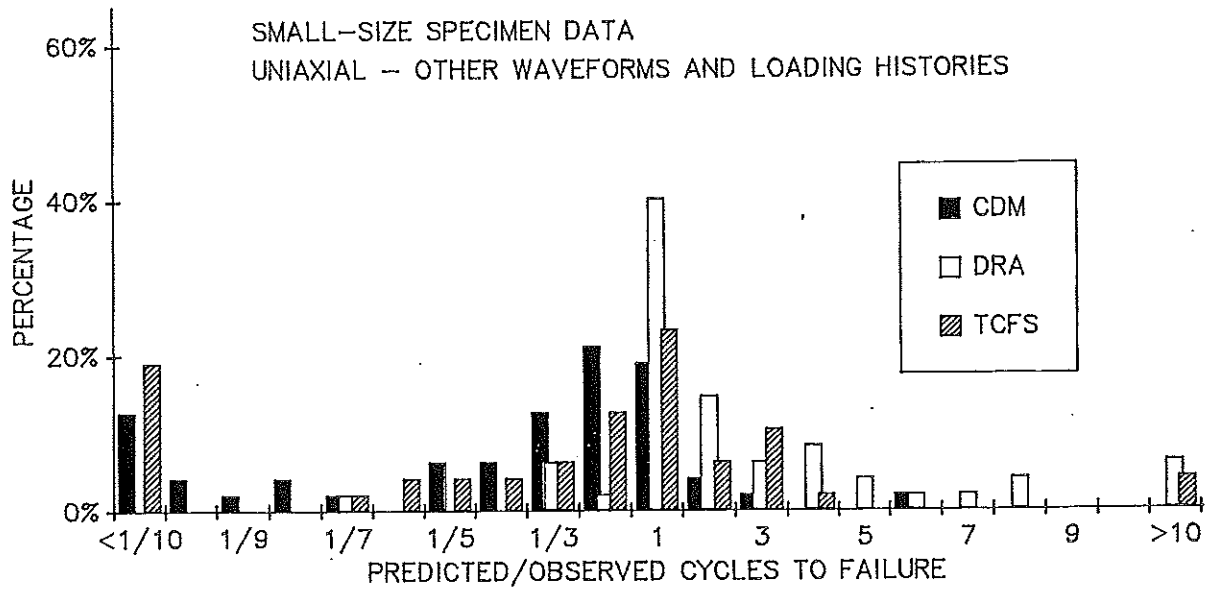


Fig.10 - Normalized distribution of predicted to observed life ratios.

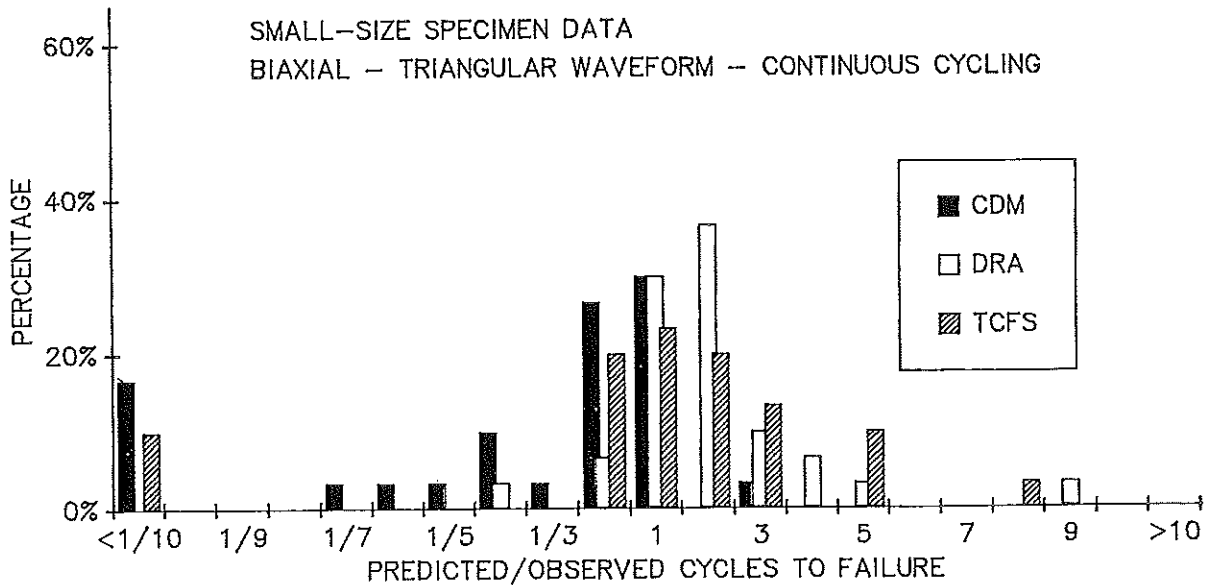


Fig.11 - Normalized distribution of predicted to observed life ratios.

When complex loading is added to biaxiality the situation changes markedly, as shown in Fig. 12: the CDM is the only method with a

correct prediction as most probable result, while the DRA most probable prediction is a factor of 3 unconservative and the TCFS has a 50% probability of being conservative for a factor greater than 10.

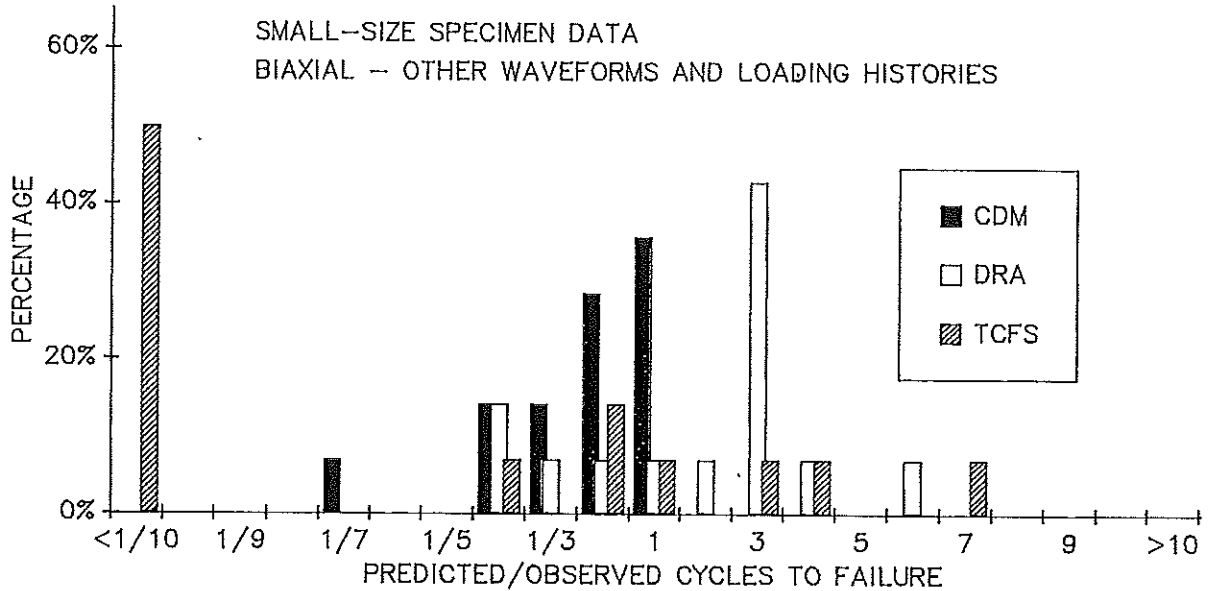


Fig.12 - Normalized distribution of predicted to observed life ratios.

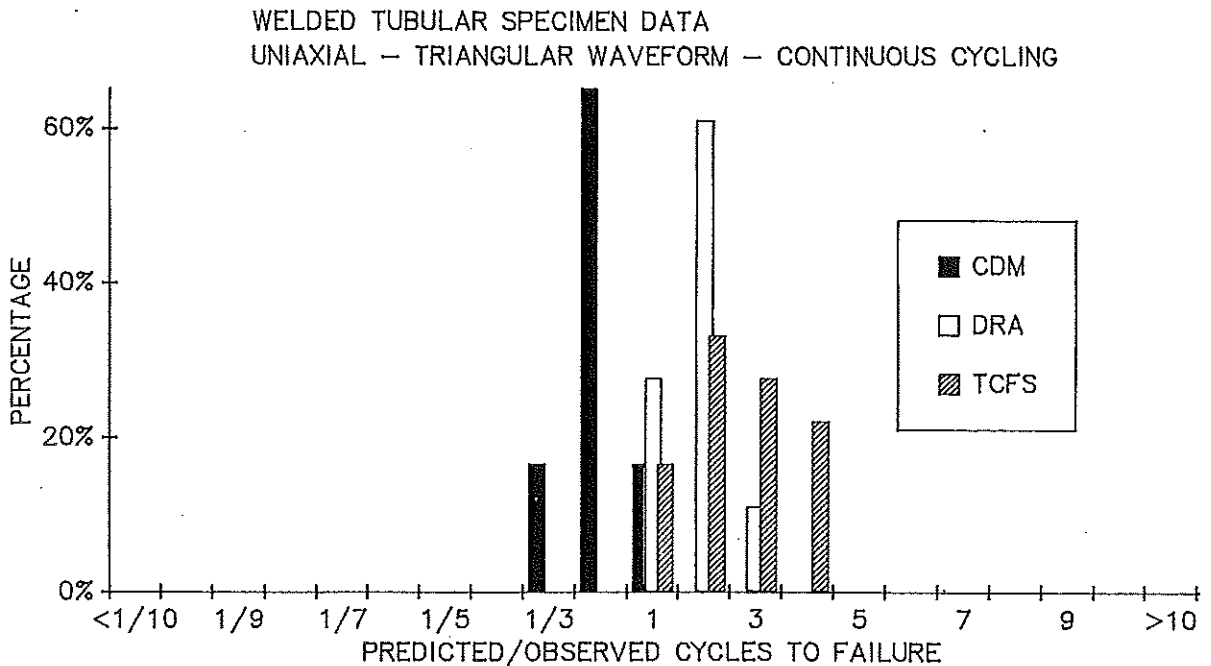


Fig.13 - Normalized distribution of predicted to observed life ratios.

The analysis of predictions made for model structures is shown in Figs. 13 and 14 for uniaxial continuous cycling and biaxial plus hold-time data, respectively. In order to obtain data representations similar to those formerly presented for small-size specimens, predictions from best and worst weld shapes were averaged, so that a single predicted value could be used for each

test. In both figures a definite trend is observed for the CDM to be overly pessimistic, all predictions falling on the conservative side. The DRA and the TCFS tend to be unconservative in predicting uniaxial continuous cycling behaviour, while the overall accuracy seems to be better for the more complex conditions of fig.14.

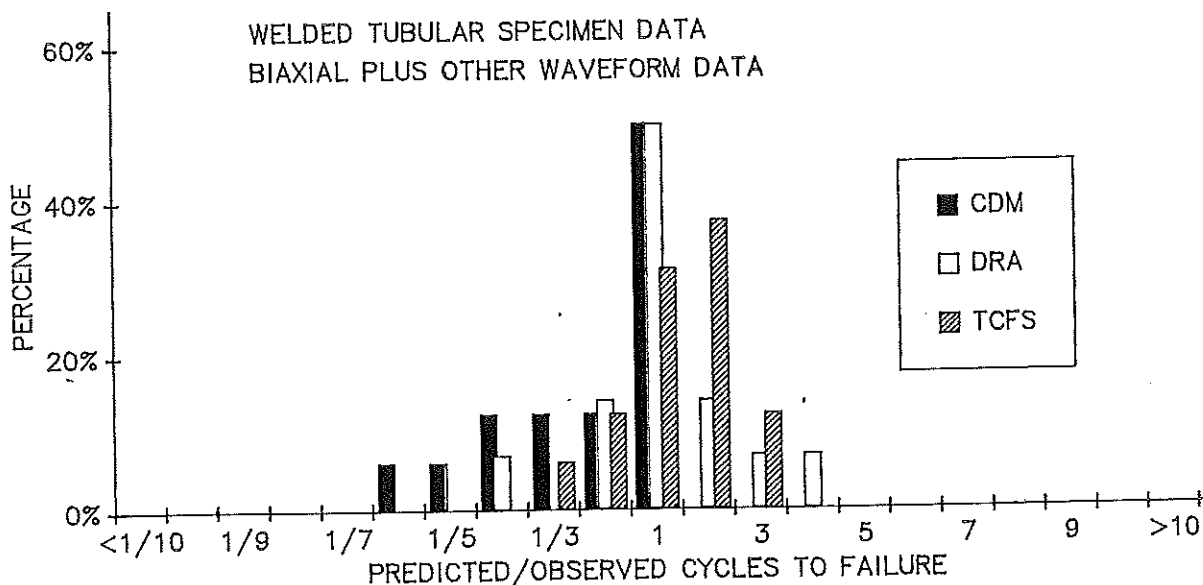


Fig.14 - Normalized distribution of predicted to observed life ratios.

While some other interesting observations could be made by a deeper and more detailed analysis of the statistical tendencies of the predictions, it seems here more worth outlining a few general conclusion that can be drawn from the work as a whole.

First of all it has to be recognized that prediction accuracy of the CDM and DRA could probably be improved if the special test results required for an accurate evaluation of material parameters were available; on the other hand the need for special and rarely available test data to obtain a proper calibration is one of the most severe shortcomings of these methods.

A significant difference has been generally observed between the CDM, which is based on stress ranges, and the other two models, which use strain components: in most cases the CDM is more conservative, especially for the shorter life durations. This may be due to a number of factors, among which the followings seem more important in the present analysis. First of all, most tests were conducted in strain control so that stress ranges had to be derived by means of available cyclic stress-strain relationships, which introduces additional uncertainty. Secondly, stress ranges varied in these tests with elapsed cycles, so that stabilized stress levels used for life prediction with CDM are an upper bound

of the actual load history. This is particularly true for high-strain/low-life tests, where most cycles are spent in strain hardening or damage softening, and for model structures, where, in addition, stabilized peak stresses are probably overestimated.

The 3-D plots of Figs. 15 and 16 may give a guidance for an overall evaluation of the present analysis. In both figures the whole of small-size specimen and model structure results have been reported as a function of load history complexity and multiaxiality. In Fig. 15 the fraction of predictions within a factor of two is shown for the 3 models, giving a comprehensive indication of their performance in terms of accuracy; it is clearly evidenced that accuracy is rapidly decreasing with increasing test complexity due either to multiaxiality or to load history or both, the DRA showing in these cases slightly better predictions as compared to the other models.

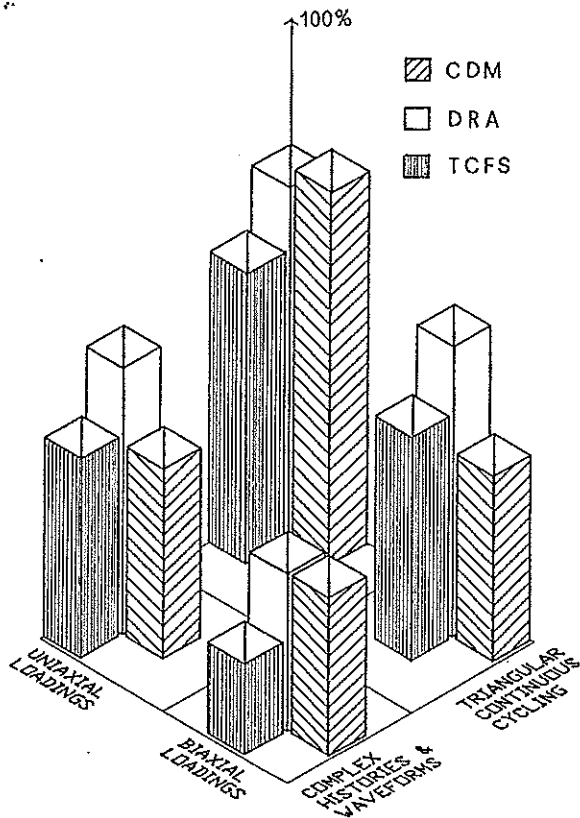


Fig.15 - Fraction of predictions within a factor of 2, as function of multiaxiality and load history complexity.

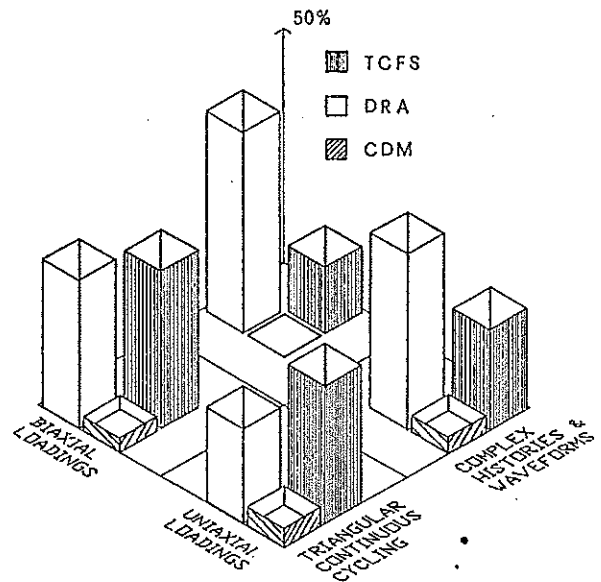


Fig.16 - Fraction of predictions unconservative for a factor greater than 2, as function of multiaxiality and load history complexity.

In Fig. 16 a similar picture is given for fractions of predictions which were unconservative for a factor greater than 2. It is particularly evidenced that the CDM has the lowest probability of being unconservative irrespective of the test complexity.

It can be suggested that graphs like those of Figs. 15 and 16, possibly based on a greater number of data and test conditions, could be used, at a design stage, in order to select an appropriate prediction methodology as function of the particular problem being examined and of specific design requirements.

Finally it seems worth of note to observe that in most cases, with reference to Figs.9-14, the envelope of the distributions obtained by single models is by far a better approximation of a normal distribution than any of the three single distributions. Were this behavior confirmed by other independent applications, it would suggest that an higher level prediction methodology could be set up, based on cumulative distributions obtained by appropriate weighting (depending on load complexity and multiaxiality) of predictions obtained by several models.

### Conclusions

On the basis of the above summarized results the following main conclusions can be derived :

1. All the three models, with parameters fitted on completely independent data, showed an high level of reliability for small-size specimens under simple loading conditions and stress states; on the other hand this reliability is significantly reduced, for all of the models, when dealing with multiaxial stresses and/or complex histories.
2. For some very complex load histories highly unconservative predictions have been found for TCFS and DRA, while CDM was extremely conservative.
3. Predictions for model structures, based on local peak stress-strain values, follow the same general trends as for small specimens, even if there is a tendency for TCFS and DRA to be somewhat unconservative, while CDM is always conservative.
4. As a rule, the CDM, which requires an evaluation of stress ranges from strain data, gives overly conservative results when dealing with high-strain tests too.
5. As a general conclusion the present analysis suggests the



possibility of using prediction distributions as guidelines for the choice of the appropriate life evaluation methodology at a design stage.

Acknowledgements

Thanks to UKAEA Risley Laboratories and INTERATOM GmbH many unpublished creep-fatigue test results were made available for this work.

Table I - Summary of test conditions for data used as basis for application of life prediction models.

	UNIAXIAL	BIAXIAL		AXIAL + PRESSURE
		IN-PHASE	OUT-OF-PHASE	
TRIANGULAR CONTINUOUS CYCLING	26-316-593	27-304-650	28-304-650	26-316-593
	27-304-650	28-304-550	304-550	
	28-304-650	29-304-650		
	304-550	(•)35-316-550		
	29-304-650			
	34-316-550			
	(•)35-316-550			
	(•)316-650			
OTHER WAVEFORMS	29-304-650	29-304-650	28-304-650	26-316-593
	31-316-570	28-304-550	304-550	
	316-550			
	34-316-550			
	26-316-593			
	30-316-600			
	28-304-650			
	304-550			
	(•)35-316-550			
	(•)316-650			
COMPLEX LOADING HISTORIES	32-316-550			
	33-316-625			
	316-600			

Legend: Reference-Material-Temperature (°C)  
(•) Tests on model structures

REFERENCES

- [1] Coffin et al. "Time Dependent Fatigue of Structural Alloys - A General Assessment" ORNL-5073 Oak Ridge, 1977
- [2] Del Puglia, Manfredi "High Temperature Low Cycle Fatigue Damage" from "Creep of Eng.Mat. and Struct." pp.229-265, Appl.Science Publ. London 1979
- [3] Bertini, Vitale "Modelization of Creep Fatigue Damage Under Complex Loading Histories and Multiaxial States of Stress"- 5th SMiRT Post-Conf. Sem. on Inel. Anal. and Life Pred. in High Temp. Fatigue, Paris, 1985.

- [4] Bertini, Vitale "Numerical Evaluation of two Creep- Fatigue Damage Models Under Complex Loading Histories and Multiaxial States of Stress", J. Press. Vess. Tech., Vol. 110, pp.97-100, February 1988.
- [5] Cailletaud et al. "A Review of Creep-Fatigue Life Prediction Methods", 7th SMIRT, Chicago, August 1983.
- [6] Inoue, Igari, Okazaki, Sakane, Tokimasa, "Fatigue-creep life prediction of 2 1/4 Cr-1 Mo steel by inelastic analysis - Result of joint work (B)", 9th SMIRT, Lausanne, 17-21 August 1987, Vol. L, pp. 261-266.
- [7] Lemaitre, Chaboche "A Non Linear Model of Creep Fatigue Damage Cumulation and Interaction", Proc.IUTAM Symposium, Gotheborg, 1974
- [8] Majumdar, Maiya "A Mechanistic Model for Time Dependent Fatigue" - J.Eng. Mat. and Struct., 1980
- [9] Anon. "ASME Boiler and Pressure Vessel Code" Code Case N47-23 "Class 1 Components in Elevated Temperature Service", ASME Publications, New York, 1986
- [10] Anon. "RCC-MR - Design and Construction Rules for Mechanical Components of FBR Nuclear Islands" AFCEN Publication, Paris, 1985
- [11] Taira "Lifetime of Structures Subjected to Varying Load and Temperature" from "Creep in Structures", Academic Press, New York, 1962
- [12] Manfredi et al. "A Review of the Creep Fatigue Interaction on AISI 304 and AISI 316 Stainless Steels" JRC Euratom ISPRA TN107018134, Ispra 1981
- [13] Chaboche "Amoragge en Fatigue a Faible ou Grand Nombre de Cycles" - Seminar du Coll.Inter. des Sciences de la Construction, St.Remy le Creveuse, 1979
- [14] Chaboche "The Concept of Effective Stress Applied to Elasticity and to Viscoplasticity in the Presence of Anisotropic Damage" - Proc.Euromec Symp. Grenoble, 1979
- [15] Kachanov "On the Time of the Rupture Process under Creep Conditions" Izvest.Akad.Nauk. SSSR, OTN Moscow 1958
- [16] Hayhurst "Creep Rupture under Multiaxial States of Stress", J. Mech. Phys. Sol., 1972, V. 20, pp. 381-390
- [17] Lemaitre, Chaboche "Mecanique des materiaux solides" Bordas, Paris, 1985
- [18] Majumdar "Designing Against Low Cycle Fatigue at Elevated Temperature" Nucl.Eng. and Des. 1981
- [19] Manfredi, Vitale "Aspects of the Creep-fatigue Problems in Materials and Structures", CEA-ENEA Seminar on Design Rules and Structure Analysis at High Temperature, Venice, September 20-22, 1982.
- [20] Manfredi, Vitale "Creep Strength and Hot Tensile Behaviour in AISI 316 Austenitic Steel", 2nd Int. Conf. on Creep and Fracture of Engineering Materials and Structures, Swansea, 1984.
- [21] Manfredi, Vitale, Bertini "Austenitic Stainless Steels Type AISI 304 and 316 under Cyclic Loads at High Temperatures", University of Pisa, Dipartimento di Costruzioni Meccaniche e Nucleari, RL 034(83), Pisa, 1983.
- [22] Carmignani, Vitale 'MAVIS-N: un programma per l'analisi di strutture a comportamento elasto-visco-plastico - Manuale di riferimento', E.T.S. Editrice, Pisa 1984.
- [23] Bertini "MADAN : un programma per l'analisi del danneggiamento da creep-fatica basato sul CDM", DCMN University of Pisa, RL112(84), 1984.
- [24] Bertini "FALT-87 : Un insieme di programmi per la previsione

- della durata in condizioni di creep-fatica" DCMN, University of Pisa, RL318(87), 1987
- [25] Bertini "A Comparison of Three Creep-Fatigue Life Prediction Models under Several Different Loading Conditions", Spec. Meet. on Creep-Fat. Damage Prediction Methods, Risley, U.K., May 1988.
- [26] Majumdar "Biaxial Cyclic Deformation and Creep-Fatigue Behavior of Materials for Solar Thermal Systems", J. Press. Vess. Tech., Vol.104, pagg. 88-95, May 1982.
- [27] Sakane et al. "Fracture Modes and Low Cycle Biaxial Fatigue Life at Elevated Temperatures", J. of Eng. Mat. and Tech., Vol.109, p.237, July 1987
- [28] Ohnami et al. "Effect of Changing Principal Stress Axes on Low Cycle Fatigue Life in Various Strain Wave Shapes at Elevated Temperatures", Multiaxial Fatigue, ASTM STP 853, 1985.
- [29] Hamada et al. "Creep-Fatigue Studies Under a Biaxial Stress State at Elevated Temperature", Fat. of Eng. Mat. and Struct., Vol.7, n.2, p.85, 1984
- [30] Clayton "UKAEA Creep-Fatigue Tests on Type 316/316L Steel Involving Compressive Dwell Periods", Priv. Comm.
- [31] Connaughton "Cumulative Damage in Creep-Fatigue Loading Tests on Type 316 Steel with Thirty Minute Dwell Periods at 550 C", Risley Nucl. Power Devel. Lab., ND-M-3343(R)
- [32] Wood et al. "A Ductility Exhaustion Evaluation of Some Long Term Creep/Fatigue Tests on Austenitic Steel", Risley Nucl. Power Devel. Lab., ND.R.1470(R)
- [33] Wood et al. "Failure Behaviour of Type 316 Steel Under Complex Faigue Cycling Conditions", Risley Nucl. Power Devel. Lab., NRL-M-1001(R)
- [34] Meurer "Compilation of Interatom Holdtime Results on 316L (N) at 550 °C", Interatom Report 55.09198.9, 1988.
- [35] Manfredi, Vitale "Elevated Temperature Low-Cycle Fatigue Strength of Butt Welded AISI 316 Steel Pipes", presented at the INTERATOM Specialist's Meeting on 'Creep and Fatigue of Weldments', Bergish Gladbach (FRG), April 28, 1987 (to be published on 'Journal of Engineering Materials and Technology', 1989).
- [36] Vitale, "Characterization of the Stress-Strain Behaviour in Type 316 Stainless Steel Welded Joints", 'Creep and Fracture of Engineering Materials and Structures' - Part II, Pineridge Press, Swansea, U.K., 1984.
- [37] Bertini, Vitale "Una modifica del metodo 'Time and Cycle Fraction Summation' per il calcolo del danneggiamento in condizioni di creep-fatica" - IIN University of Pisa, RP404(80), 1980.